Published in final edited form as:
Langmuir. 2009 October 6; 25(19): 11467–11471. doi:10.1021/la901239v.

Phase Separation at the Surface of Poly(ethylene oxide)-Containing Biodegradable Poly(L-lactic acid) Blends

Jinxiang Yu[†], **Christine M. Mahoney**[‡], **Albert J. Fahey**[‡], **Wesley L. Hicks Jr.**[§], **Robert Hard**[‖], **Frank V. Bright**[†], and **Joseph A. Gardella**[†,*]

[†]Department of Chemistry, State University of New York, Buffalo, New York 14260

[‡]Analytical Microscopy Group, Surface and Microanalysis Science Division, National Institute of Standards and Technology, Gaithersburg, Maryland 20899

[§]Department of Head and Neck Surgery, Roswell Park Cancer Institute, Buffalo, New York 14263

[‖]Department of Anatomy/Cell Biology, State University of New York, Buffalo, New York 14214

Abstract

The surface chemistry and in-depth distribution of the composition of a poly(ethylene oxide) (PEO)-containing biodegradable poly(L-lactic acid) (PLLA) blend matrix system have been investigated using X-ray photoelectron spectroscopy (XPS). This study reports detailed quantitative compositional information using a novel numerical method for determining depth profiles. The PEO system studied is an amphiphilic Pluronic P104 surfactant, PEO–*b*-poly(propylene oxide) (PPO)–*b*-PEO. The extent of phase separation is analyzed by determining the surface enrichment of the PEO component via measurement of chemical composition at the polymer–air interface. For this blend system, the combination of the PPO component in the Pluronic surfactants drives the formation of a surface excess of Pluronic in the blends with PLLA. The surface excess profile shows a rapid increase in Pluronic surface composition versus bulk Pluronic mass fractions of 1–5%, but the profile levels off above bulk Pluronic mass fractions of 5%.

Introduction

Poly(ethylene oxide) (PEO) is a neutral, highly biocompatible, and pharmacologically inactive water-soluble polymer.[1] The incorporation of PEO into biodegradable poly(L-lactic acid) (PLLA)-based drug delivery implant systems is expected to improve the interfacial biocompatibility of these polymeric devices.[2] Blend matrices of PEO in relatively hydrophobic PLLA should improve the three-dimensional stability and the biological activity of water-soluble macromolecular drugs such as proteins or enzymes in the delivery systems, which are incorporated into the matrix.[3] There are two reasons for this. (1) Surface-segregated PEO in the aqueous environment provides a diffusive hydrophilic layer[4] facilitating the interaction between cells and polymeric biodevices, and (2) the hydrophilic PEO segments in the bulk can protect water-soluble drugs from hydrophobic polymers in the form[5] of a micelle or encapsulation.

A model system of PEO-containing polymer systems that are candidates for including protein-based drugs into the PLLA matrix is to use PEO–*b*-poly(propylene oxide) (PPO)–*b*-PEO triblock copolymers, e.g., Pluronic surfactants. Pluronics exhibit a wide range of

*To whom correspondence should be addressed. gardella@acsu.buffalo.edu.

hydrophilicity and hydrophobicity as a function of the PEO/PPO ratio.[6] Blends can exhibit advantageous physicomechanical properties that each individual polymer does not have.[7,8] The chemistry of this polymer system has been extensively studied. However, few studies have reported surface characteristics. For example, Park et al.[9] postulated from the scanning electron microscopy (SEM) study of PLLA/Pluronic blend systems that Pluronics might be entangled within the amorphous domains of PLLA, while the PPO segments might be anchored on PLLA spherulites. Pluronic L101, recommended by Park et al.,[9] contains a high content of PPO, which is not as biocompatible as PEO. A surfactant with a lower PPO content, Pluronic P104, is used in this study. In this report, we quantify in depth the phase separation phenomena using angle-dependent X-ray photoelectron spectroscopy (AD-XPS) for surface composition profiles.

Experimental Section

Materials

Poly(L-lactic acid) (MW = 100000) was purchased from Polysciences Inc. (Warrington, PA).[10] Pluronic P104 (H_2O solubility of >10%, MW = 5900, PEO mass fraction of 40%) was kindly donated by BASF Corp.[6] (Mount Olive, NJ). Glass coverslips (22 mm in diameter, cleaned) were purchased from Fisher Scientific Corp. (Hanover Park, IL) as substrates. HPLC grade chloroform was purchased from Aldrich (Milwaukee, WI). Reagent grade *n*-hexane (Fisher Scientific) and methanol (Fisher Scientific) for cleaning were used as received without further purification. The sample names, component structures, uses, and bulk compositions are listed in Table 1, where the compositions are listed in terms of mass fractions of the P104 component (χ_{P104}). Each concentration of polymer thin films was fabricated by spin-casting (model EC 101 spin-coater, Headway Research Inc., Garland, TX) the corresponding solution onto three to six glass coverslips at 1500 rpm for 60 s. The spin-cast samples were immediately vacuum-dried in a vacuum oven (model 5830 vacuum oven, National Appliance Co., Portland, OR) at room temperature under reduced pressure (107 Pa or 0.8 Torr) for at least 24 h. The spin-cast procedure was conducted according to the guidelines of Frank et al.[11] and Xie et al.[12] The blend film thicknesses were 600–900 nm: some were measured by a profilometer (alpha-step 200, Tencor Instruments, Milpitas, CA) employing a 9.81×10^{-5} N (10 mg) stylus force; the others were estimated by scanning electron microscopy (SEM) images. The pure P104 films were the thinnest (≈500 nm). For annealing, some samples were selected for placement in 100 or 250 mL flasks with vacuum stopper joints. The flasks were then connected to a vacuum line and pumped down to ≤20 Pa (0.15 Torr). The flasks were kept at 70–80 °C for at least 24 h.

X-ray Photoelectron Spectroscopy

Surface chemical compositions were obtained using a Physical Electronic PHI 5300 X-ray photoelectron spectrometer equipped with a hemispherical energy analyzer. An achromatic Mg Kα X-ray source (1253.6 eV) was operated at 15 kV and 20 mA. The energy analyzer was operated at a pass energy of 89.45 eV for survey acquisitions as well as 35.75 or 17.90 eV for high-resolution acquisitions. The energy resolution was 0.1 eV with a 20 eV energy range for high-resolution spectra, or 1.0 eV for survey spectra. The C_{1s} and O_{1s} envelopes were used for all angle-dependent acquisitions. The acquisition time was within 1 h without observed damage of the samples, which was evidenced by the lack of change in the sample color and the lack of difference between the first and last high-resolution spectra, which were acquired at the same takeoff angle. The operating pressure of XPS was $<4.0 \times 10^{-6}$ Pa (3.0×10^{-8} Torr), and the background pressure was $<1.2 \times 10^{-6}$ Pa (9.0×10^{-9} Torr). Binding energies were calibrated by setting the CH_x peak in the C_{1s} envelope at 285.0 eV. Photoelectron emission takeoff angles (relative to the surface) of 15°, 30°, 45°, and 90° were used for all samples and led to sampling depths of ≈2.7, 5.0, 7.3, and 10.3 nm for the C_{1s}

envelope, respectively.[13] Each composition at each takeoff angle was measured between three and six times using identical sample types. Each sample was used for only one run. Curve fitting was performed for each carbon fraction of C–H_x, C–O, and O–C═O functionalities using AugerScan version 2.41 (RBD Enterprises, Bend, OR). Before curve fitting, all C_{1s} envelopes were background subtracted. They were curve fit with a Gaussian–Lorentzian band type. The limits used to curve fitting were as follows: binding energy ± 0.2 eV, fwhm ± 0.10 eV, and % Gauss = 10%. Quantitative analysis of pure Pluronic P104 samples can be accomplished by evaluation of the C–O/CH_x fractions because of the difference in the PPO block versus PEO block. Quantitative analysis of the blends will be presented below in a separate section. An XPS instrument equipped with an Al Kα monochromatic X-ray source and with a hemispherical energy analyzer was used for experiments with the annealed sample. Its other conditions were the same as those mentioned above.

Quantitative XPS Calculations

The structures of P104 and PLLA and other information are listed in Table 1. We define

$$X=x+x' \quad (1)$$

where X is the sum of the monomer numbers of two PEO blocks in P104. The monomer mass of LLA (M_{LLA}) in the blends is 72.06 g/mol. The average monomer mass of P104 in the blends (M_{P104}) depends on the molar ratio of PEO to PPO in P104 ($r = X/y$, where the definition of y is in Table 1). The molar percentage of PEO in P104 composition in blends is

$$\frac{X}{X+y}=\frac{r}{r+1} \quad (2)$$

A curve fitting result for the C_{1s} envelope in an XPS high-resolution spectrum of the poly(L-lactic acid)/Pluronic P104 blend (sample 8020) is shown in Figure 1. The peaks were assigned as follows: peak a (O═C–O) at ≈289.5 eV, peak b (C–O) at ~286.7 eV, and peak c (C–H_x) at 285.0 eV. After curve fitting, the area fraction of each peak was determined.

In the blend system, several percentages were defined for convenient use: molar percentage of PLLA at sampling depth, z; molar percentage of P104 at sampling depth, $1 - z$; mass fraction of PLLA at sampling depth, p; mass fraction of P104 at sampling depth, $1 - p$. From Table 2 and eqs 3–10, the surface mass fractions of P104 were calculated and the results were verified. From Table 2, the C_{1s} envelope curve fitting method:

$$\mathrm{O=C-O\,area\%}=a=\frac{z(r+1)}{rz+2r+3} \quad (3)$$

$$\mathrm{CH}_x\mathrm{\,area\%}=c=\frac{rz+1}{rz+2r+3} \quad (4)$$

From Table 2, the atomic molar ratio method:

$$\mathrm{C/O}=1.5z+2\frac{r(1-z)}{r+1}+3\frac{(1-z)}{r+1}$$

Rewrite this equation:

$$\mathrm{C/O}=\frac{6+4r-3z-rz}{2(r+1)} \quad (5)$$

Dividing eq 3 by eq 4 and then solving it, we have

$$r=X/y=-1 \text{ or } \frac{-3c+1}{2(c-a)} \quad (6)$$

(obviously −1 does not have physical meaning and is rejected) and

$$z=\frac{2a}{1-c} \quad (7)$$

Then rewrite eq 5 to have an equation to verify the accuracy of curve fitting:

$$\mathrm{C/O}=\frac{6a^2+3ac-7a-2c+2}{c^2+2ac-2a-2c+1} \quad (8)$$

The C/O ratio was also provided by AugerScan after the XPS experiments and the background subtraction operations. Equation 8, however, is the calculated result from the curve fitting of the C_{1s} high-resolution spectra. Therefore, comparison of this calculated value with the ratio provided by AugerScan becomes a verification method of curve fitting accuracy. If the measured C/O ratio is different from the calculated result of eq 8, curve fitting is redone. The average monomer weight of P104 in the blends is

$$\overline{M_{\mathrm{P104}}}=\frac{44X+58y}{X+y}=\frac{44r+58}{r+1} \quad (9)$$

The mass fraction of PLLA at the particular sampling depth in the blends is given by

$$p=\frac{36a-36ac-72a^2}{4c^2-14a^2+ac-15a-15c+11} \quad (10)$$

and the mass fraction of P104 at sampling depth in the blends equals 1 − *p*.

XPS Depth Profile Reconstruction

For each type of sample, a hypothetical composition depth profile was convolved with an exponential function that describes the decreasing intensity of photoelectrons in XPS with depth. Using this function, XPS theoretical intensity ratios were calculated at each takeoff angle and compared to the experimental ratios. The hypothetical composition depth profile was then varied until the error between calculated and measured ratios was minimized. The composition depth profile, *v*(*l*), can be described by

$$\begin{aligned} v(l)&=C_{\mathrm{surf}} && 0<l\le x \\ v(l)&=\frac{C_{\mathrm{surf}}-HC_{\mathrm{bulk}}}{2}\left\{1+\cos\left[\frac{\pi(1-x)}{L-x}\right]\right\}+HC_{\mathrm{bulk}} && x<l\le L \\ v(l)&=\left\{\left[1+(H-1)\mathrm{e}^{-0.5\left(\frac{l-L}{S_2}\right)^2}\right]C_{\mathrm{bulk}}\right\} && L<l \end{aligned} \quad (11)$$

This function describes the changing mass fraction of P104 with depth (l) and is a modified version of algorithms developed previously,[14–21] where C_{bulk} is the bulk mass fraction of P104, C_{surf} is the surface mass fraction of P104, H is the fraction ($0 < H < 1$) of C_{bulk} located at the minimum of the function, L is the depth (l) where this minimum is located, S_2 is a parameter which defines the shape of the curve after the minimum, and x describes the location of the first inflection point in the graph, where the mass fraction starts to decrease to its minimum. When l is less than x, the normalized mass fraction $v(l)$ is set as C_{surf}, while after that point, $v(l)$ varies with l.

The optimization process was performed using subroutines written in C++ (Borland 5.0). The subroutines use a duplicate simplex method to directly search for the closest match between the convoluted data calculated from the profiles and the XPS experimental data. This is done by varying of the five parameters defined above (H, L, S_2, x, and C_{surf}) such that the lowest standard error value is obtained between experimental and calculated data. Unlike previous optimization methods, this method provides visual displays of the standard error values, such that rapid optimization can be achieved.

Results and Discussion

We investigated the surface segregation of PPO within pure Pluronic P104 using XPS and found that the C–O peak percentage in the C_{1s} envelope changed from 70.5, 75.5, 78.6, and 80.7% at takeoff angles of 15°, 30°, 45°, and 90°, respectively. This indicates that in pure P104 samples PPO is segregated to the topmost surface of the film. Notice that the area fraction of the C–O peak at 90° takeoff angle was close to the theoretical value for bulk[22,23] (C–O peak area fraction ≈ 80%). This also was consistent with the segregation PPO to the topmost layers. The integrity of the film was also checked by SEM images (Figure 2). The increase in the level of P104 surfactant in bulk resulted in some “bubbles” at the thin film surface. The cross sections (broken at liquid nitrogen temperature) had a morphology similar to those of the surfaces.

Figure 3 plots surface compositions of the PLLA/P104 films as determined by XPS, as a function of known bulk composition. Four major results were noted in this study. (1) No points were on the unit line. Therefore, surface segregation of P104 exists at all bulk compositions and takeoff angles. (2) The P104 surface concentration increased markedly with the increase in P104 bulk concentration: at a 15° takeoff angle (TOA), the first five blends (χ_{P104}= 1, 2, 3, 4, and 5%) showed markedly increasing level of segregation with increasing bulk P104 content (surface contents of 7.2 and 47.4% for bulk contents of 1 and 5%, respectively), while the last nine blends (χ_{P104} = 10–50%) were found to increase at a much slower rate with increasing P104 bulk concentration (surface contents of 55.7 and 81.4% for bulk contents of 10 and 50%, respectively), as shown in Figure 3. This indicates that the sample surface concentration of P104 quickly increased when the bulk P104 concentration increased to 5%; after that, the surface P104 concentration remained essentially the same even after we increased the bulk concentration to 50% of P104. (3) Data at three different takeoff angles (15°, 30°, and 90°) of each blend were used for measurements; the level of segregation at 15° was the largest and then that at 30°, and 90° had equivalent surface compositions (this indicated a depletion zone beneath the surfactant-enriched zone). All samples were also investigated at a 45° TOA (data not shown), and they displayed an almost overlapping line with the 90° line. Such a compositional trend was also observed in TOF-SIMS depth profiling.[24] For example, a depletion region was observed immediately after the surface-enriched P104 region. Since the sampling depth of XPS is only 1–10 nm, our XPS experimental results could never fully depict the broad depletion region, which was indicated by TOF-SIMS depth profiling (~730 Å from the air surface for blend 7525).[24] (4) The difference between 15° and 30° was larger than the difference

between 30° and 90°, indicating that the level of segregation was greater at the topmost surface than at the deeper regions. This was also consistent with what was observed from the XPS reconstructed depth profiles (Figure 4) and the TOF-SIMS depth profiling.[24] Figure 4 indicates at the surface up to 1.5 nm, the P104 surfactant concentrations were 20 and 50% when the bulk concentrations were 2 and 5%, respectively. Then a zone having a P104 concentration even lower than the bulk concentration exists from 1.5 to >10.5 nm. We call the first zone (0–1.5 nm) the enriched zone; the second zone (from 1.5 to >10.5 nm) is called the depletion zone.

Low-mass and high-mass portions of TOF-SIMS spectra were acquired and have been published.[25] Those TOF-SIMS spectra indicated the same description given above. In other words, PPO is the driving force that leads the the segregation of surfactant onto the surface in the PLLA/Pluoronic blend system.

The equilibrium blend system was checked by annealing several blend films in vacuum at 70–80 °C, which is above the glass transition temperatures of all three components in the blend (PEO, PPO, and PLLA). The P104 surface compositions (χ_{P104}) at 45° TOA were 19.3, 28.9, and 59.7%for fresh blends and 17.2, 29.1, and 59.7% for annealed blends of 9802, 9505, and 7525, respectively, which were acquired by another XPS (see Experimental Section). This system is an equilibrium system. Since these were thick films (400–900 nm), no interference of the interfaces (the air–polymer interface and the polymer–substrate interface) with each other was expected, which was also evidenced by the TOF-SIMS depth profiling.[24]

Conclusions

The phase separation was investigated at the surface of PEO-containing biodegradable PLLA blends. The enrichment of the component was determined in detail at the polymer–air interface through the XPS studies. For the blend system, the combination of the PPO component in the Pluronic surfactants drives the formation of a surface excess of Pluronic in the blends with PLLA. The surface excess profile shows a rapid increase in surface composition versus bulk composition for samples containing 1–5% (χ_{P104}), but the profile levels off from 5 to 50%. The results show the topmost surface layer comprised the initial addition of Pluronic, followed by a more gradual increase likely due to increases in the bulk distribution of Pluronic.

Acknowledgments

We acknowledge support from the National Science Foundation Analytical and Surface Chemistry program.

References

1. Ronneberger B, Kao WJ, Anderson JM, Kissel T. J. Biomed. Mater. Res. 1996; 30:31–40. [PubMed: 8788103]
2. Uhrich KE, Cannizzaro SM, Langer RS, Shakesheff KM. Chem. Rev. 1999; 99:3181–3198. [PubMed: 11749514]
3. Lee J-W, Gardella Joseph A Jr. Anal. Bioanal. Chem. 2002; 373:526–537. [PubMed: 12185564]
4. Yang Z, Galloway JA, Yu H. Langmuir. 1999; 15:8405–8411.
5. Emoto K, Nagasaki Y, Kataoka K. Langmuir. 1999; 15:5212–5218.
6. Florham Park, NJ: BASF Corp.; 2004. http://www.basf.com/static/OpenMarket/Xcelerate/Preview_cid-982931199931_pubid-974236729499_c-Article.html;
7. Krause, S. Polymer Blends. Paul, DR.; Newman, S., editors. Vol. Vol. 1. New York: Academic Press; 1978. p. 15

8. Park A, Wu B, Griffith LG. J. Biomater. Sci. Polym. Ed. 1998; 9:89–110. [PubMed: 9493839]
9. Park TG, Cohen S, Langer R. Macromolecules. 1992; 25:116–122.
10. Certain commercial equipments, instruments, or materials are identified in this article to specify adequately the experimental procedure. Such identification does not imply recommendation or endorsement by the National Institute of Standards and Technology, nor does it imply that the materials or equipment identified is necessarily the best available for the purpose.
11. Frank CW, Rao V, Despotopoulou MM, Pease RFW, Hinsberg WD, Miller RD, Rabolt JF. Science. 1996; 273:912–915. [PubMed: 8688068]
12. Xie F, Zhang HF, Lee FK, Du B, Tsui OKC, Yokoe Y, Tanaka K, Takahara A, Kajiyama T, He T. Macromolecules. 2002; 35:1491–1492.
13. Zhao J, Rojstaczer SR, Gardella JA Jr. J. Vac. Sci. Technol., A. 1998; 16:3046–3051.
14. Mahoney CM, Gardella JA Jr, Rosenfeld JC. Macromolecules. 2002; 35:5256–5266.
15. Zhuang H, Marra KG, Ho T, Chapman TM, Gardella JA Jr. Macromolecules. 1996; 29:1660–1665.
16. Gardella JA Jr, Ho T, Wynne KJ, Zhuang H-Z. J. Colloid Interface Sci. 1995; 176:277–279.
17. Zhuang, H.; Marra, KG.; Ho, T.; Chapman, TM.; Gardella, JA, Jr. Government Report Announcement Index. New York: University of New York; 1995. p. 31TR-95-05
18. Zhao J, Rojstaczer SR, Chen J, Xu M, Gardella JA Jr. Macromolecules. 1999; 32:455–461.
19. Chen X, Gardella JA Jr, Kumler PL. Macromolecules. 1992; 25:6621–6630.
20. Chen X, Gardella JA Jr, Ho T, Wynne KJ. Macromolecules. 1995; 28:1635–1642.
21. Mittlefehldt ER, Gardella JA Jr, Salvati L Jr. Anal. Chim. Acta. 1986; 191:227–241.
22. Rastogi AK, St. Pierre LE. J. Colloid Interface Sci. 1969; 31:168–175.
23. O'Connor SM, Deanglis AP, Gehrke SH, Retzinger GS. Biotechnol. Appl. Biosci. 2000; 31(Part 3):185–196.
24. Mahoney CM, Yu J, Gardella JA Jr. Anal. Chem. 2005; 77:3570–3578. [PubMed: 15924391]
25. Lee JW, Jeong ED, Cho EJ, Gardella JA Jr, Hicks W Jr, Hard R, Bright FV. Appl. Surf. Sci. 2008; 255:2360–2360.

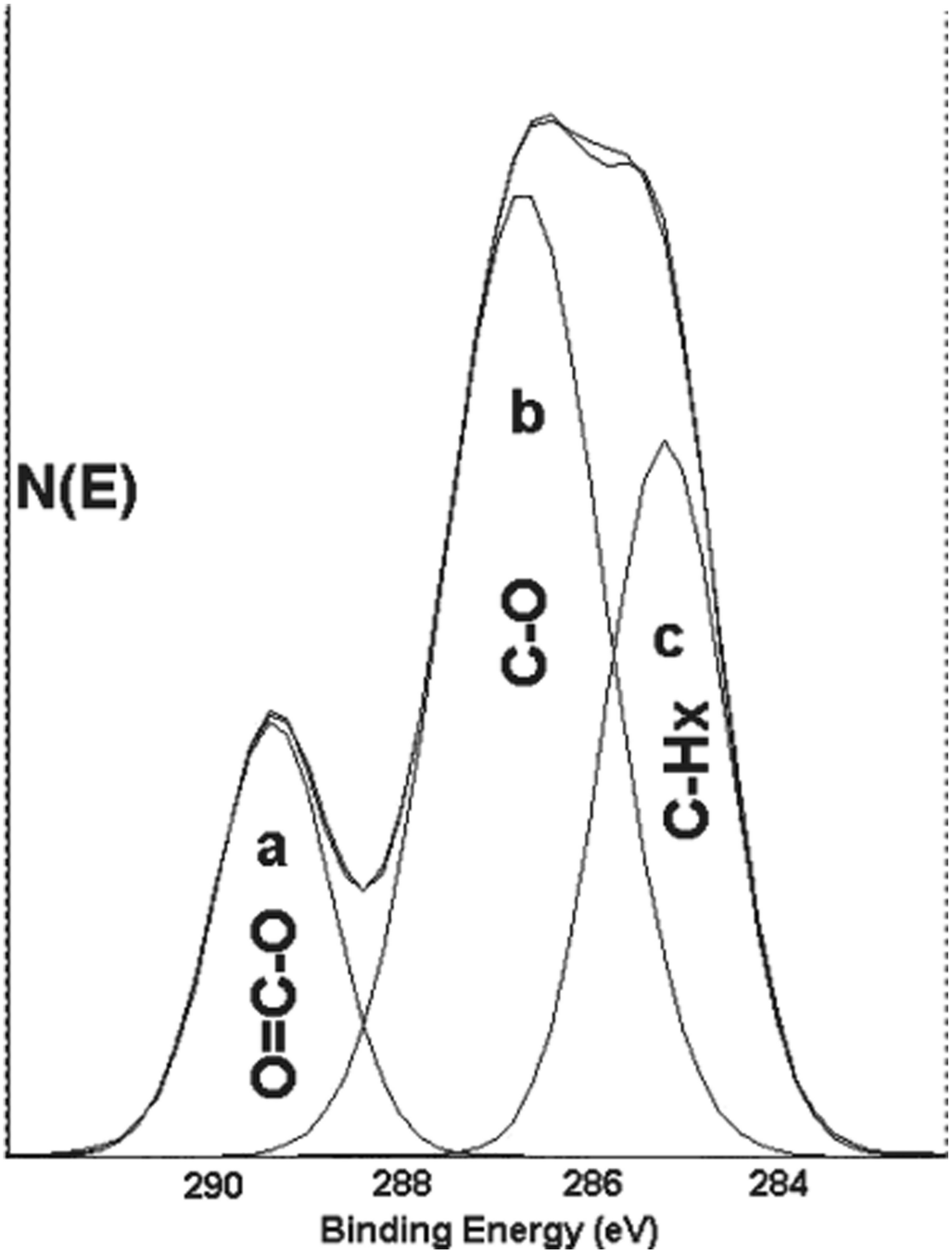

Figure 1.
Curve fitting results for the C_{1s} envelope in an XPS high-resolution spectrum of a poly(L-lactic acid)/Pluronic P104 blend (8020).

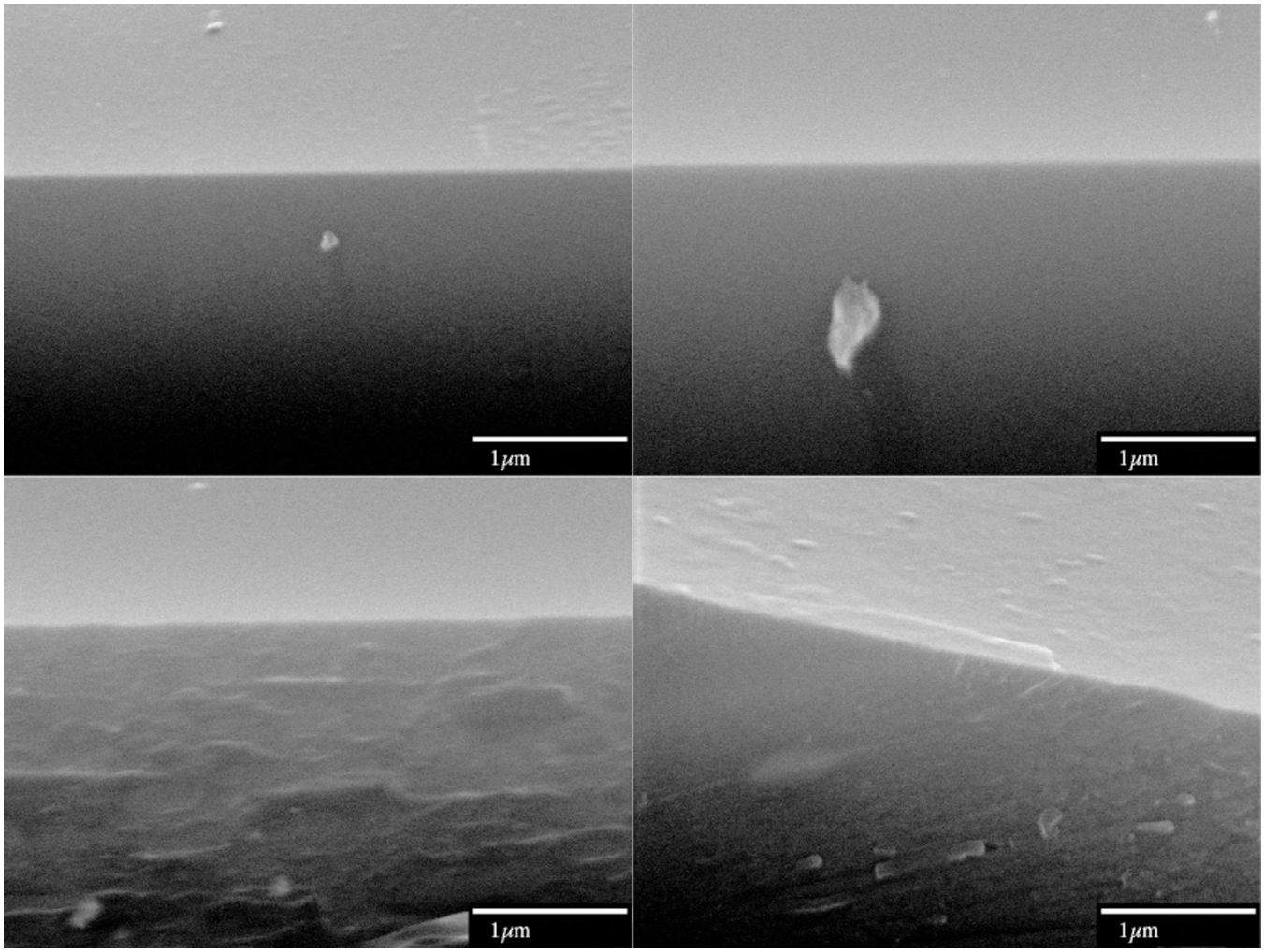

Figure 2.
SEM images of 9802 (top left), 9505 (top right), 9010 (bottom left), and 7030 (bottom right).

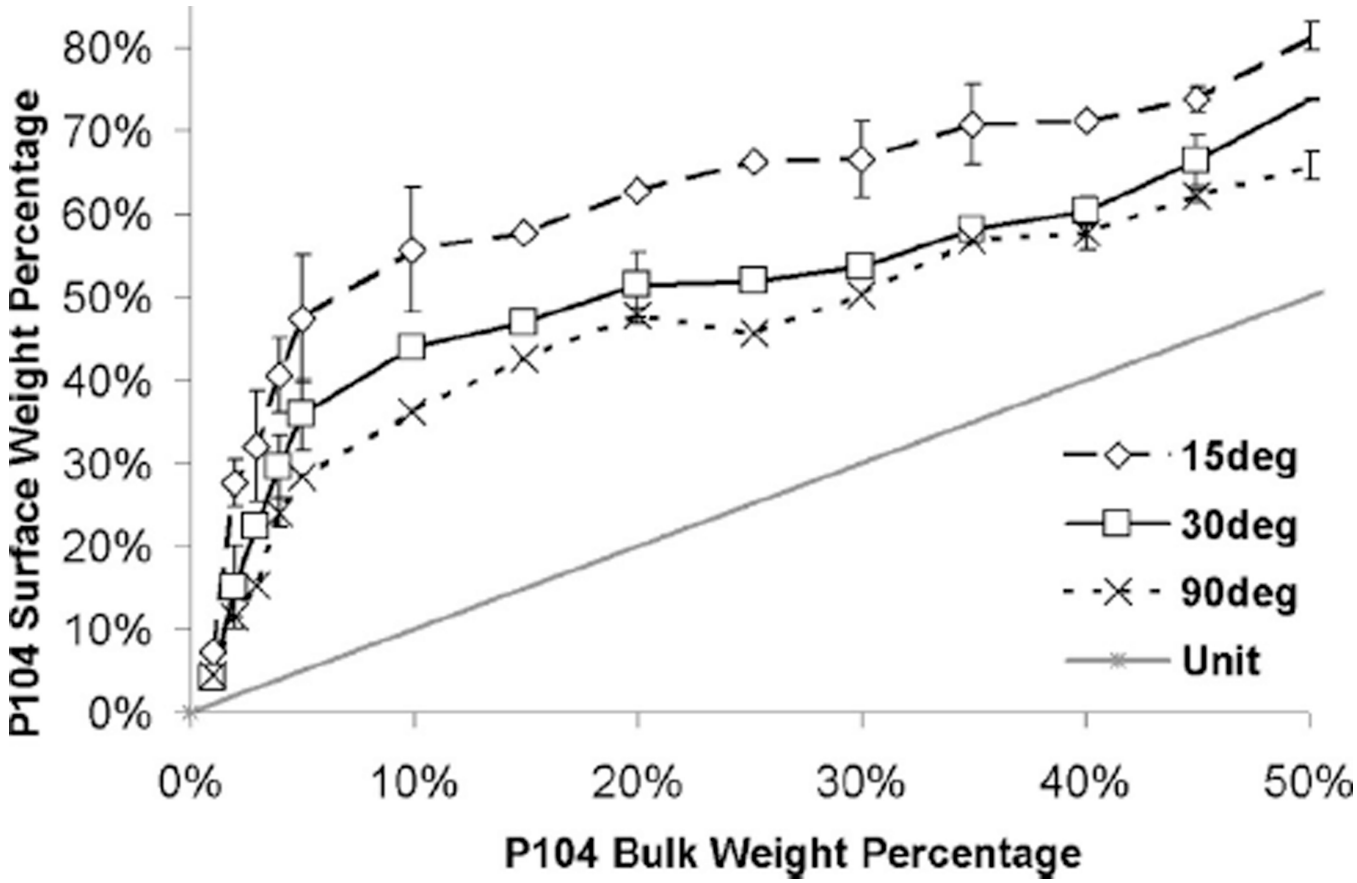

Figure 3.
Effect of Pluronic P104 bulk mass fraction on surface mass fraction in blend samples: (◇) takeoff angle of 15°, (□) takeoff angle of 30°, (×) takeoff angle of 90°, and (*) unit line. The error bars represent standard deviations.

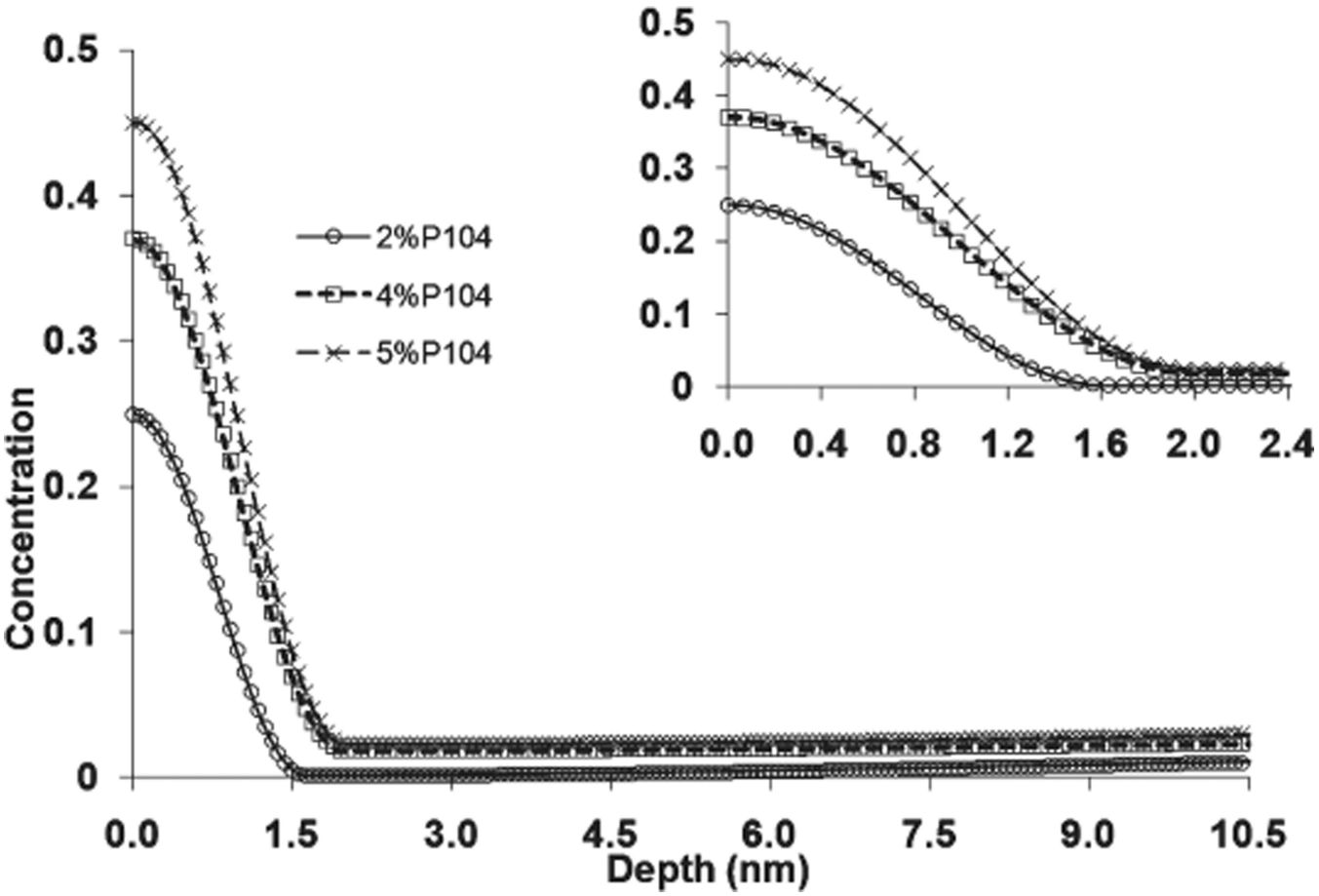

Figure 4.
Concentration depth profiles (CDPs) reconstructed from angle-dependent XPS experiments with PLLA/P104 blends.

Table 1

Bulk Composition, Uses, and Component Structures of 16 Samples Used in This Study

sample type[a]	P104 mass fraction (χ_{P104}) (%)	uses/structures
PLLA		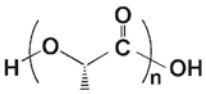
PLLA	0.0	AD-XPS, TOF-SIMS depth profiling, TOF-SIMS
9901	1.0	AD-XPS, TOF-SIMS depth profiling
9802	2.0	AD-XPS, TOF-SIMS depth profiling, XPS CDP reconstruction, SEM, comparison between annealed and fresh samples
9703	3.0	AD-XPS
9604[b]	4.0	AD-XPS, TOF-SIMS depth profiling, XPS CDP reconstruction
9505	5.0	AD-XPS, TOF-SIMS depth profiling, XPS CDP reconstruction, SEM, comparison between annealed and fresh samples
9010	9.9	AD-XPS, TOF-SIMS depth profiling, TOF-SIMS, SEM
8515	14.9	AD-XPS
8020	20.0	AD-XPS, TOF-SIMS
7525	25.2	AD-XPS, TOF-SIMS depth profiling, comparison between annealed and fresh samples
7030	30.0	AD-XPS, TOF-SIMS, SEM
6535	34.9	AD-XPS
6040	40.0	AD-XPS
5545	44.9	AD-XPS
5050	50.0	AD-XPS
P104	100.0	AD-XPS, TOF-SIMS depth profiling, TOF-SIMS, SEM
P104		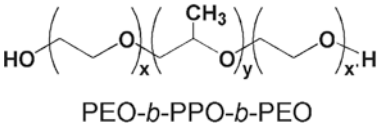 PEO-*b*-PPO-*b*-PEO

[a] We prepared all samples by dissolving the two polymers into 10 mL of chloroform, spin-casting to form thin films, and then vacuum drying.

[b] All samples except sample type 9604 have a solvate/solvent ratio of 0.03 g/mL. Sample type 9604 has a solvate/solvent ratio of 0.032 g/mL.

Table 2

Relationships between Components in the Blends to Peaks in the C_{1s} Envelope and the Carbon to Oxygen Molar Ratios in the Monomers[a]

	C_{1s} envelope curve fitting method				atomic molar ratio method
blend composition	**O═C–O peak**	**C–O peak**	**C–H_x peak**	**sum**	**C/O**
$PLLA_n$	z	z	z	_[b]	1.5
PPO_y	0	$2(1 - z)/(r + 1)$	$(1 - z)/(r + 1)$	_[b]	2
PEO_x	0	$2r(1 - z)/(r + 1)$	0	_[b]	3
sum	z	$2 - z$	$(rz + 1)/(r + 1)$	$(rz + 2r + 3)/(r + 1)$	_[b]

[a] Three equations were developed from these data. Two were used for calculation, and one was used for verification: O═C–O area % = $a = (zr + z)/(rz + 2r + 3)$, CH_X area % = $c = (rz + 1)/(rz + 2r + 3)$, and $C/O = (6 + 4r - 3z - rz)/(2r + 2)$.

[b] Not used for equations.